Published in final edited form as:
J Tissue Eng Regen Med. 2009 August ; 3(6): 486–490. doi:10.1002/term.183.

Initial Evaluation of Vascular Ingrowth into Superporous Hydrogels

Vandana Keskar[1], **Milind Gandhi**[1], **Ernest J. Gemeinhart**[1], and **Richard A. Gemeinhart**[1,2,3,*]

[1]Department of Biopharmaceutical Sciences, University of Illinois, Chicago, IL 60612-7231, USA

[2]Department of Bioengineering, University of Illinois, Chicago, IL 60612-7052, USA.

[3]Department of Ophthalmology and Visual Science, University of Illinois, Chicago, IL 60612-4319, USA.

Abstract

There is a need of new materials and architectures for tissue engineering and regenerative medicine. Based upon our recent results developing novel scaffold architecture, we hypothesized that this new architecture would foster vascularization, a particular need for tissue engineering. We report on the potential of superporous hydrogel (SPH) scaffolds for *in vivo* cellular infiltration and vascularization. Poly(ethylene glycol) diacrylate (PEGDA) SPH scaffolds were implanted in the dorsum of severe combined immunodeficient (SCID) mice and harvested after four weeks of *in vivo* implantation. The SPHs were visibly red and vascularized as apparent when compared to the non-porous hydrogel controls which were macroscopically avascular. Host cell infiltration was observed throughout the SPHs. Blood cells and vascular structures, confirmed through staining for CD 34 and smooth muscle alpha actin, were observed throughout the scaffolds. This novel soft material may be utilized for cell transplantation, tissue engineering, and in combination with cell therapies. The neovascularization and limited fibritic response suggest that the architecture may be conducive to cell survival and rapid vessel development.

Keywords

hydrogel; pore; scaffold; poly(ethylene glycol) diacrylate; *in vivo*; vascularization

Tissue engineering, which applies the principles of biology and engineering to the development of functional substitutes for damaged tissues or organs (Langer, 1997), has been increasingly discussed as an option to overcome limitations of transplanting tissues. While *in vitro* tissue engineered constructs consist of cells seeded on suitable scaffolds with minimal mortality, *in vivo* cells within these constructs cannot survive by diffusion alone (Folkman, 1995) and constructs must support angiogenesis. Angiogenesis within scaffolds also allows successful engraftment of the construct into the surrounding host tissue (Rucker et al., 2006). To this end, porous hydrogel scaffolds are being investigated (Druecke et al., 2004; Ford et al., 2006; Wake et al., 1994).

The inherent hydrated architecture of synthetic hydrogels imparts mechanical properties similar to soft tissues and extracellular matrix (Peppas et al., 2000) which are natural hydrogels. Natural and synthetic hydrogels have been extensively examined and applied to hard and soft tissue even when the hydrogel is significantly weaker than the bulk tissue (Lee

*To whom correspondence should be addressed, 833 S. Wood St., Chicago, IL 60612-7231. rag@uic.edu. Tel.: +1(312) 996-2253. Fax: +1(312) 996-2784..

and Mooney, 2001; Yamamoto et al., 2000). The hydrophilicity, favorable biological recognition properties, and the ability to encapsulate cells within the hydrated network (Burdick and Anseth, 2002; Elisseeff et al., 1999) have suggested the applicability of poly(ethylene glycol) diacrylate (PEGDA) hydrogels for tissue engineering constructs (Nguyen and West, 2002). Additionally, various strategies have been reported to modulate the degradation of PEGDA scaffolds which typically aim for degradation of the scaffold in concert with new tissue growth (Hudalla et al., 2008; Kim et al., 2008; Kraehenbuehl et al., 2008). However, the photopolymerization techniques which are commonly used for preparation of non-porous hydrogels, have the disadvantages of relatively large diffusion distances and limited cell-cell interactions within the scaffolds (Nuttelman et al., 2004). While the rate and depth of vascular ingrowth into scaffolds are influenced by the presence, size, and interconnectivity of pores (Druecke et al., 2004; Gerecht et al., 2007; Landers et al., 2002), engineering interconnected porous architectures within hydrogels is a challenge. Various techniques have been employed for generating a porous architecture (Flynn et al., 2003; Ford et al., 2006; Landers et al., 2002; Liu et al., 2000; Weinand et al., 2007; Yoon et al., 2004), but interconnected pores are not always formed. Without interconnected pores or inherent degradability, cell penetration and proliferation within the scaffolds is inhibited (Chirila et al., 1993). In addition to pores being necessary for cell invasion, surface modification, either by conjugating peptides with cell adhesive sequences (Hern and Hubbell, 1998; Hersel et al., 2003) or infiltrating the hydrophobic scaffold with a hydrophilic polymer, have been proposed to be required to make hydrophilic scaffolds conducive to cell attachment and migration (Mooney et al., 1995). To this end, hydrophilic polyvinyl alcohol (PVA) sponges have been extensively studied as *in vivo* models for wound healing and foreign body reaction (Diegelmann et al., 1986; Kyriakides and Bornstein, 2003). While early stages (1-3 weeks) of cell invasion into the PVA sponge is characterized by neo-vascularization, the later stages (3 weeks) of the response are typical of a foreign body response leading to a fibrotic encapsulation (Kyriakides and Bornstein, 2003; Nam et al., 2004). Formation of this avascular and acellular fibrous capsule can be deleterious to the function of a tissue engineered construct. The implant cannot further vascularize and the cells within the implant undergo ischemic death (Anderson, 2006). Additionally, PVA sponges as implant scaffolds require pro-angiogenic factors (Yamamoto et al., 2000) or implantation in the highly vascular mesenteric space of a larger animal model to ensure vascularization (Takeda et al., 1995). This limits the use of PVA sponges for long term implantation and cell encapsulation.

Our group has recently reported that unmodified PEGDA superporous hydrogels (SPH) allow human mesenchymal stem cell loading, survival for up to a month and stimuli-induced differentiation (Keskar et al.). PEGDA SPHs are highly permeable due to its high water content that which may hold advantages over hydrophobic polymer-based scaffolds. With these observations, we hypothesized that the highly interconnected porous architecture would be favorable for cellular infiltration and angiogenesis *in vivo*. We further hypothesized that the limited fibrotic response to nonporous PEGDA-based hydrogels would be similar when the porous network was implanted.

PEGDA (MW 3400 g/mol) SPH scaffolds were prepared and characterized as previously reported (Keskar et al.). Briefly, PEGDA solution, foam stabilizer (Pluronic™ F127, double distilled water, the initiator pair, N,N,N’,N’- tetramethylethylene-diamine (TEMED) and ammonium persulfate, were added sequentially to a glass vial. Saturated citric acid solution was used for pH adjustment. The precursor solution was mixed and heated gently to 37°C for approximately 2 minutes. Sodium bicarbonate, 200 mg, was added with constant stirring to evenly distribute the salt and evolving gas. The SPHs were then removed from the vial and allowed to swell in double distilled water to remove traces of unpolymerized monomers and salt before dehydrating in 80% ethanol followed by overnight dehydration in absolute

ethanol. The hydrogels were then dried in a food dessicator and stored in an airtight container for further use. To make the non-porous PEGDA hydrogels (NPH), sodium bicarbonate, 200 mg, was replaced with sodium hydroxide solution. The precursor solution was pipetted into 96 well plates with each well containing an equivalent volume to the size of the total volume of the porous hydrogel. Polymerization was allowed to proceed for half an hour. The NPHs were then rinsed with double distilled water to remove traces of unpolymerized monomers, dried and stored in an airtight container for further use. Scanning electron microscopy of the interior surface of the dehydrated SPHs revealed interconnected pores ranging from 100 μm to 600 μm with an average pore size of 250 ± 94 μm (Fig. 1a). The hydrated SPH had a larger pore diameter and broader distribution in pore diameter, 395 ± 107 μm, as estimated from bright field images (Fig. 1b).

To investigate the potential of the SPHs for *in vivo* angiogenesis, the SPHs were implanted in the dorsal skin fold of SCID mice (Fox Chase SCID, Charles River Laboratories). SCID mice were chosen as the model for vascularization as part of a larger experimental design involving human cells incorporated within the SPH where the tissue growth and vascularization within the SPH will be evaluated. All animal experiments were approved by the institutional animal care committee at the University of Illinois at Chicago. Experimental design for the study was developed using power analysis of published data of porous polymer implants (Arinzeh et al., 2005; Hidetsugu et al., 2007). Briefly, the mice were divided into 2 groups of 7 mice each. The mice were anesthetized with intraperitoneal injection of 100 mg/kg ketamine and 5 mg/kg xylazine. Subcutaneous pockets were opened in the back of the mice using a blunt probe. Two hydrogels, either SPH or NPH, were inserted within either side of the pocket. The incision was closed and the animals were monitored for four weeks. At the end of four weeks, the mice were sacrificed by an overdose of carbon dioxide followed by cervical dislocation. The hydrogels were removed *en bloc*. Fixed samples were placed in paraffin, sectioned and processed further for histological evaluation of cellular infiltration and vascular ingrowths.

Upon implantation, the hydrogels could be palpated easily. Daily monitoring did not reveal any weight loss or any apparent signs of toxicity like inflammation or reddening of skin in the test animals. At the end of four weeks, the hydrogels could be seen attached to the inside of the dorsal skin. Gross appearance revealed the red, vascularized superporous hydrogels (Fig. 2a) and the pale yellow avascular non-porous hydrogels (Fig. 2b). Hematoxylin and eosin (H&E) staining of the SPH sections revealed host cell infiltration throughout the scaffold (Fig. 3a) which was absent in the nonporous hydrogels. Thus, the porous architecture of the SPH seemed to provide a favorable environment for micro-vessel formation. While it has previously been demonstrated that the rate and the depth of vascular ingrowths within scaffolds are influenced by the presence of pores (Gerecht et al., 2007) the number of vascular ingrowths are limited by the interconnectivity of the pores within the scaffolds (Druecke et al., 2004;Landers et al., 2002).

To further elucidate the presence of host cells, paraffin embedded sections were de-paraffinized in xylene, hydrated with serial concentrations of ethanol and stained with Hoechst 33258 nuclear stain (Latt and Stetten, 1976) (Fig. 3b). A fibrotic, vascularized capsular layer surrounding the SPH was formed (Fig. 4). Extracted SPH implants showed the presence of blood cells and vascular structures. A representative image taken from the center of the SPH section revealed the presence of these ingrowths to the core of the SPH (Fig. 5a). Lumen-like structures filled with blood cells (Fig. 5b) confirmed the presence of a functional microvasculature.

To further confirm the presence of microvasculature, CD34, an early stage endothelial cell marker (Civin et al., 1990), and alpha smooth muscle actin (α-SMA), a vascular smooth

muscle cell marker (Van Gieson et al., 2003), were examined. Briefly, the de-paraffinized and hydrated sections were blocked with 1% bovine serum albumin in phosphate buffered saline (pH 7.4) for 30 minutes. The sections were then incubated with primary rat polyclonal antibodies against CD34 and mouse polyclonal antibodies against smooth muscle α-actin (Santa Cruz Biotechnology) for 2 hrs followed by incubation with FITC conjugated goat anti rat and goat anti mouse (Molecular Probes) respectively for 30 mins. Hoechst 33258 was used as the nuclear stain. CD34 positive endothelial cells were localized throughout the SPHs (Fig. 6a). In addition, vessel lining musculature (Owens, 1995) was observed in the form of α-SMA positive cells, associated with the vascular growths (Fig. 6b). These results suggest that the ingrowths observed within the implanted acellular SPHs are neo-vasculature.

Conclusion

Tissues generated *in vitro* or *in vivo* must survive and function *in vivo* However, *in vivo* tissue viability and function is limited by the ability of the scaffold to support functional microvasculature and overcome subsequent transport limitations. The unmodified PEGDA SPHs utilized in this study were able to support initial *in vivo* vascularization upon implantation in SCID mice. The presence of a highly interconnected porous architecture within the PEGDA SPH provided an open network which facilitated cellular infiltration from the host and vascular ingrowth throughout the scaffold; PEGDA scaffolds with discontinuous pores should, however, be employed in future studies to elucidate the importance of pore interconnectivity and the rate of *in vivo* vascularization. In summary, we present a platform scaffold technology that should be further examined for tissue engineering applications. The approach of *in vivo* implantation of the acellular SPH or seeding cells within the SPH scaffolds before *in vivo* implantation, could both benefit from rapid thorough vascularization. Future studies will be directed at further understanding the dynamics of vascular infiltration and the stability of the newly formed vasculature.

Acknowledgments

This investigation was conducted in a facility constructed with support from Research Facilities Improvement Program Grant C06 RR15482 from the National Center for Research Resources, NIH. The authors also thank Dr. Howard Greisler for insightful comments and suggestions.

References

Anderson, JM. Tissue Engineering and Artificial Organs. In: Bronzino, JD., editor. The Biomedical Engineering Handbook. Third ed. CRC Press; Boca Raton: 2006. p. 36-35.

Arinzeh TL, Tran T, McAlary J, Daculsi G. A comparative study of biphasic calcium phosphate ceramics for human mesenchymal stem-cell-induced bone formation. Biomaterials. 2005; 26(17): 3631–3638. [PubMed: 15621253]

Burdick JA, Anseth KS. Photoencapsulation of osteoblasts in injectable RGD-modified PEG hydrogels for bone tissue engineering. Biomaterials. 2002; 23(22):4315–4323. [PubMed: 12219821]

Chirila TV, Constable IJ, Crawford GJ, Vijayasekaran S, Thompson DE, Chen YC, Fletcher WA, Griffin BJ. Poly(2-hydroxyethyl methacrylate) sponges as implant materials: in vivo and in vitro evaluation of cellular invasion. Biomaterials. 1993; 14(1):26–38. [PubMed: 7678755]

Civin CI, Strauss LC, Fackler MJ, Trischmann TM, Wiley JM, Loken MR. Positive stem cell selection--basic science. Prog Clin Biol Res. 1990; 333:387–401. [PubMed: 1689854]

Diegelmann RF, Lindblad WJ, Cohen IK. A subcutaneous implant for wound healing studies in humans. J Surg Res. 1986; 40(3):229–237. [PubMed: 3951219]

Druecke D, Langer S, Lamme E, Pieper J, Ugarkovic M, Steinau HU, Homann HH. Neovascularization of poly(ether ester) block-copolymer scaffolds in vivo: long-term investigations

using intravital fluorescent microscopy. J Biomed Mater Res A. 2004; 68(1):10–18. [PubMed: 14661244]

Elisseeff J, Anseth K, Sims D, McIntosh W, Randolph M, Yaremchuk M, Langer R. Transdermal photopolymerization of poly(ethylene oxide)-based injectable hydrogels for tissue-engineered cartilage. Plast Reconstr Surg. 1999; 104(4):1014–1022. [PubMed: 10654741]

Flynn L, Dalton PD, Shoichet MS. Fiber templating of poly(2-hydroxyethyl methacrylate) for neural tissue engineering. Biomaterials. 2003; 24(23):4265–4272. [PubMed: 12853258]

Folkman J. Angiogenesis in cancer, vascular, rheumatoid and other disease. Nat Med. 1995; 1(1):27–31. [PubMed: 7584949]

Ford MC, Bertram JP, Hynes SR, Michaud M, Li Q, Young M, Segal SS, Madri JA, Lavik EB. A macroporous hydrogel for the coculture of neural progenitor and endothelial cells to form functional vascular networks in vivo. Proc Natl Acad Sci U S A. 2006; 103(8):2512–2517. [PubMed: 16473951]

Gerecht S, Townsend SA, Pressler H, Zhu H, Nijst CL, Bruggeman JP, Nichol JW, Langer R. A porous photocurable elastomer for cell encapsulation and culture. Biomaterials. 2007; 28(32): 4826–4835. [PubMed: 17692371]

Hern DL, Hubbell JA. Incorporation of adhesion peptides into nonadhesive hydrogels useful for tissue resurfacing. J Biomed Mater Res. 1998; 39(2):266–276. [PubMed: 9457557]

Hersel U, Dahmen C, Kessler H. RGD modified polymers: biomaterials for stimulated cell adhesion and beyond. Biomaterials. 2003; 24(24):4385–4415. [PubMed: 12922151]

Hidetsugu T, Paola RA, Hitoshi N, Mehmet G, Jin LY, Borkosky SS, Liliana M, Noriyuki N. Mechanism of bone induction by KUSA/A1 cells using atelocollagen honeycomb scaffold. J Biomed Sci. 2007; 14(2):255–263. [PubMed: 17061146]

Hudalla GA, Eng TS, Murphy WL. An approach to modulate degradation and mesenchymal stem cell behavior in poly(ethylene glycol) networks. Biomacromolecules. 2008; 9(3):842–849. [PubMed: 18288800]

Keskar V, Marion NM, Mao JJ, Gemeinhart RA. In Vitro Evaluation of Macroporous Hydrogels to Facilitate Stem Cell Infiltration, Growth and Mineralization. Tissue Engineering. DOI: 10.1089=ten.tea.2008.0238.

Kim J, Lee KW, Hefferan TE, Currier BL, Yaszemski MJ, Lu L. Synthesis and evaluation of novel biodegradable hydrogels based on poly(ethylene glycol) and sebacic acid as tissue engineering scaffolds. Biomacromolecules. 2008; 9(1):149–157. [PubMed: 18072747]

Kraehenbuehl TP, Zammaretti P, Van der Vlies AJ, Schoenmakers RG, Lutolf MP, Jaconi ME, Hubbell JA. Three-dimensional extracellular matrix-directed cardioprogenitor differentiation: systematic modulation of a synthetic cell-responsive PEG-hydrogel. Biomaterials. 2008; 29(18): 2757–2766. [PubMed: 18396331]

Kyriakides TR, Bornstein P. Matricellular proteins as modulators of wound healing and the foreign body response. Thromb Haemost. 2003; 90(6):986–992. [PubMed: 14652628]

Landers R, Hubner U, Schmelzeisen R, Mulhaupt R. Rapid prototyping of scaffolds derived from thermoreversible hydrogels and tailored for applications in tissue engineering. Biomaterials. 2002; 23(23):4437–4447. [PubMed: 12322962]

Langer R. Tissue engineering: a new field and its challenges. Pharm Res. 1997; 14(7):840–841. [PubMed: 9244137]

Latt SA, Stetten G. Spectral studies on 33258 Hoechst and related bisbenzimidazole dyes useful for fluorescent detection of deoxyribonucleic acid synthesis. J Histochem Cytochem. 1976; 24(1):24–33. [PubMed: 943439]

Lee KY, Mooney DJ. Hydrogels for tissue engineering. Chem. Rev. 2001; 101(7):1869–1879. [PubMed: 11710233]

Liu Q, Hedberg EL, Liu Z, Bahulekar R, Meszlenyi RK, Mikos AG. Preparation of macroporous poly(2-hydroxyethyl methacrylate) hydrogels by enhanced phase separation. Biomaterials. 2000; 21(21):2163–2169. [PubMed: 10985489]

Mooney DJ, Park S, Kaufmann PM, Sano K, McNamara K, Vacanti JP, Langer R. Biodegradable sponges for hepatocyte transplantation. J Biomed Mater Res. 1995; 29(8):959–965. [PubMed: 7593039]

Nam SY, Nho YC, Hong SH. Evaluations of Poly(vinyl alcohol)/Alginate Hydrogels Cross-linked by γ -ray Irradiation Technique. Macromol Res. 2004; 12(2):219–224.

Nguyen KT, West JL. Photopolymerizable hydrogels for tissue engineering applications. Biomaterials. 2002; 23(22):4307–4314. [PubMed: 12219820]

Nuttelman CR, Tripodi MC, Anseth KS. In vitro osteogenic differentiation of human mesenchymal stem cells photoencapsulated in PEG hydrogels. J Biomed Mater Res A. 2004; 68(4):773–782. [PubMed: 14986332]

Owens GK. Regulation of differentiation of vascular smooth muscle cells. Physiol Rev. 1995; 75(3): 487–517. [PubMed: 7624392]

Peppas NA, Bures P, Leobandung W, Ichikawa H. Hydrogels in pharmaceutical formulations. Eur J Pharm Biopharm. 2000; 50(1):27–46. [PubMed: 10840191]

Rucker M, Laschke MW, Junker D, Carvalho C, Schramm A, Mulhaupt R, Gellrich NC, Menger MD. Angiogenic and inflammatory response to biodegradable scaffolds in dorsal skinfold chambers of mice. Biomaterials. 2006; 27(29):5027–5038. [PubMed: 16769111]

Takeda T, Murphy S, Uyama S, Organ GM, Schloo BL, Vacanti JP. Hepatocyte Transplantation in Swine Using Prevascularized Polyvinyl Alcohol Sponges. Tissue Engineering. 1995; 1(3):253–262. [PubMed: 19877904]

Van Gieson EJ, Murfee WL, Skalak TC, Price RJ. Enhanced smooth muscle cell coverage of microvessels exposed to increased hemodynamic stresses in vivo. Circ Res. 2003; 92(8):929–936. [PubMed: 12663481]

Wake MC, Patrick CW Jr. Mikos AG. Pore morphology effects on the fibrovascular tissue growth in porous polymer substrates. Cell Transplant. 1994; 3(4):339–343. [PubMed: 7522866]

Weinand C, Gupta R, Weinberg E, Madisch I, Jupiter JB, Vacanti JP. Human shaped thumb bone tissue engineered by hydrogel-beta-tricalciumphosphate/poly-epsilon-caprolactone scaffolds and magnetically sorted stem cells. Ann Plast Surg. 2007; 59(1):46–52. discussion 52. [PubMed: 17589259]

Yamamoto M, Tabata Y, Kawasaki H, Ikada Y. Promotion of fibrovascular tissue ingrowth into porous sponges by basic fibroblast growth factor. J Mater Sci Mater Med. 2000; 11(4):213–218. [PubMed: 15348034]

Yoon JJ, Song SH, Lee DS, Park TG. Immobilization of cell adhesive RGD peptide onto the surface of highly porous biodegradable polymer scaffolds fabricated by a gas foaming/salt leaching method. Biomaterials. 2004; 25(25):5613–5620. [PubMed: 15159077]

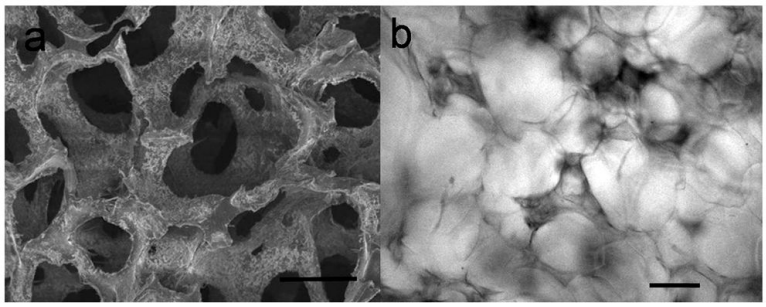

Fig. 1.

Interconnected porous architecture can be seen where each pore was internally connected to the adjacent pores. (a) Representative scanning electron micrograph of the interior of dried PEGDA SPHs. (b) Representative light micrograph of the interior of a hydrated PEGDA SPH. Scale bar in both the images is 200 μm.

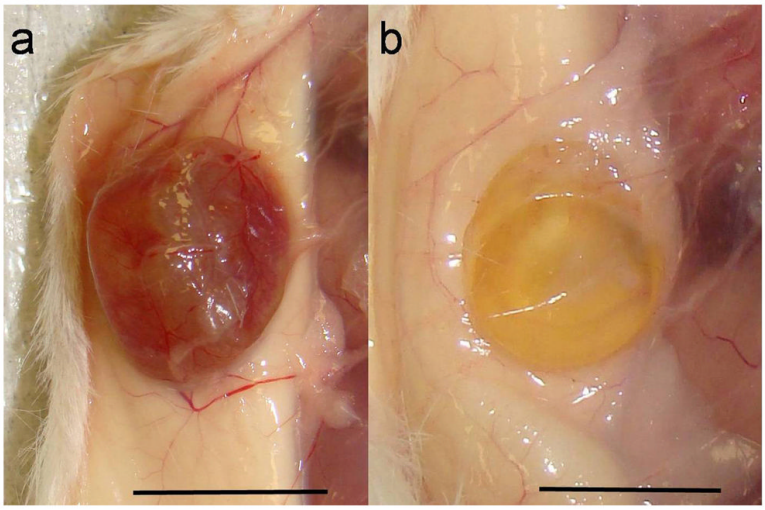

Fig. 2.

Gross images of the hydrogels extracted after 4 weeks of subcutaneous implantation in the back of SCID mice. (a) Superporous hydrogel attached to the skin, red in appearance, indicating possible vascularization. A very thin fibrous layer can be seen enclosing the SPH. (b) In comparison, the non-porous hydrogel appears avascular. In both images, the pale skin (at the center) and muscles (at the edge), are apparent. Scale bar on both the images is 1 cm.

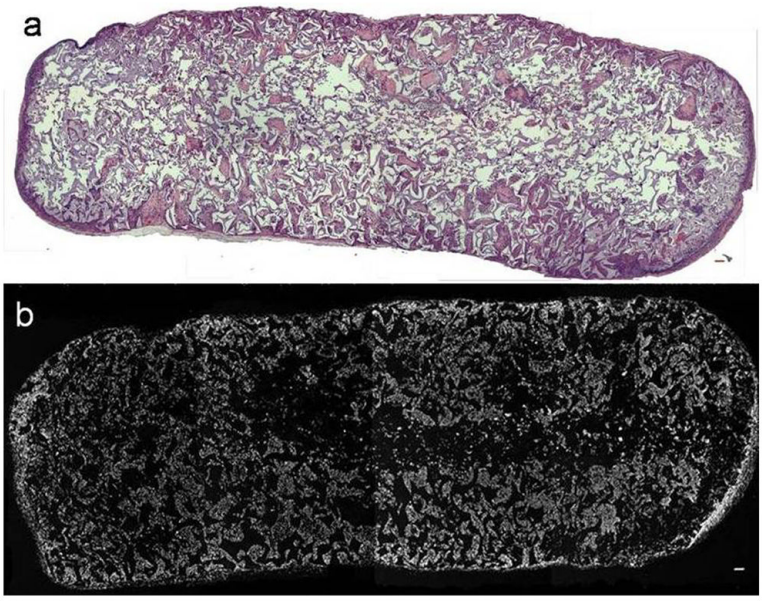

Fig. 3.

(a) H& E stained sections of the hydrogel taken from the center of the scaffold. Cellular infiltration (purple nuclei and pink cytoplasm) can be seen throughout the SPH, indicating that the host cells were able to penetrate right up to the core. (b) Combined epifluorescent images of H33258 staining within the SPH. Scale bar is 100 μm for both the images.

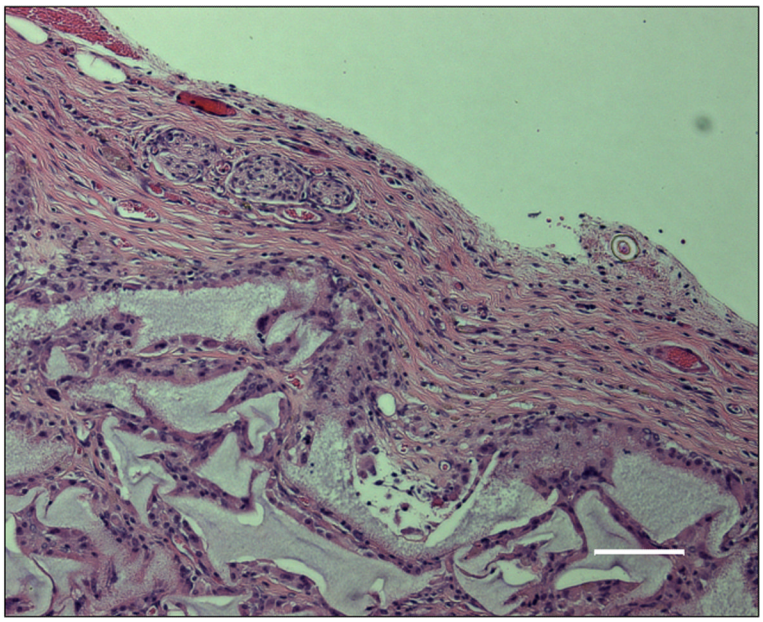

Fig. 4.
H&E section of the thin vascularized fibrotic tissue seen encapsulating the SPH, scale bar 100 μm.

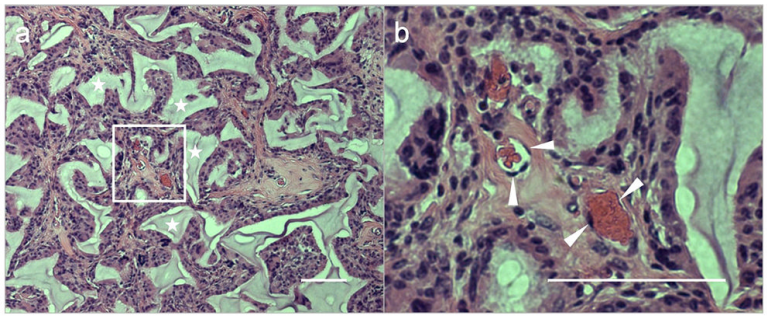

Fig. 5.

H&E staining within the SPH sections showing presence of vascular ingrowths. (a) Representative image showing extensive host cell infiltration and areas of vascularization within the SPH (*). The hydrogel sections have a faint staining and have dehydrated and thus pulled away from the cells. (b) A higher magnification image of the area highlighted in (a) clearly shows the endothelial lining of the microvessels stained blue (marked by white arrows) and the lumen filled with bright red, anucleated blood cells. Scale bar is 100 μm for both the images.

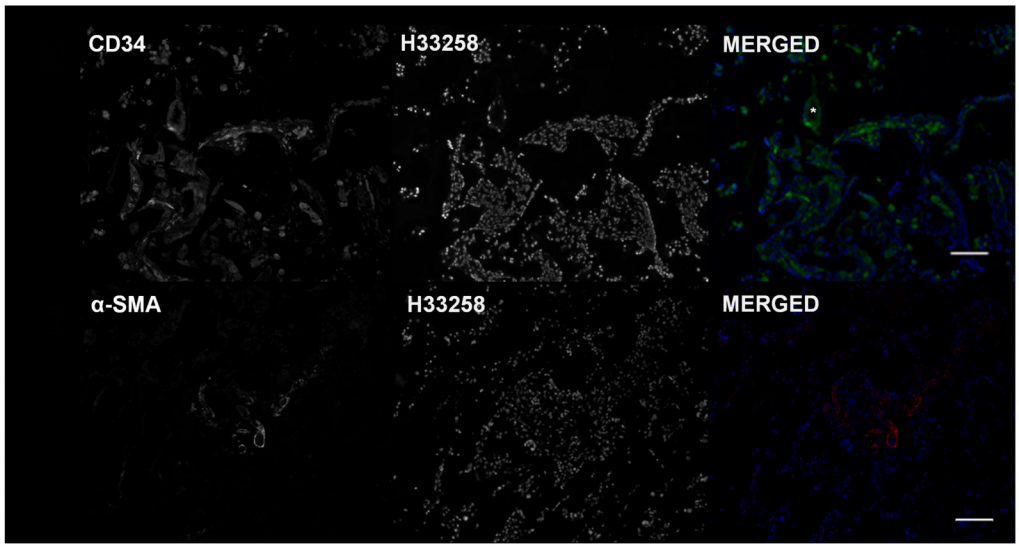

Fig. 6.

Immunohistochemical analysis of the SPH sections. (a) CD34+ endothelial cells can be seen throughout the sections with a lumen (*) clearly seen. (b) The microvessels stain positive for smooth muscle α-actin (red), indicating mature blood vessels. In both the panels, H33258 is used as the nuclear stain and scale bar is 100 μm.